Theoretical Perspectives on Proton-Coupled Electron Transfer Reactions

SHARON HAMMES-SCHIFFER*

Department of Chemistry, The Pennsylvania State University, 152 Davey Laboratory, University Park, Pennsylvania 16802

Received August 24, 2000

ABSTRACT

This Account presents a theoretical formulation for proton-coupled electron transfer reactions. The active electrons and transferring protons are treated quantum mechanically, and the free energy surfaces are obtained as functions of collective solvent coordinates corresponding to the proton and electron transfer reactions. Rate expressions have been derived in the relevant limits, and methodology for including the dynamical effects of the solvent and protein has been developed. This theoretical framework allows predictions of rates, mechanisms, and kinetic isotope effects for proton-coupled electron transfer reactions.

Introduction

Proton-coupled electron transfer (PCET) reactions play a vital role in a wide range of chemical and biological processes. For example, PCET is required for the conversion of energy in photosynthesis and respiration.[1,2] In particular, the coupling between the proton motion and electron transfer plays a key role in the proton pumping mechanism of photosynthetic reaction centers, as well as in the conduction of electrons in cytochrome *c*. PCET is also important in numerous enzyme reactions such as those of ribonucleotide reductase and iron−sulfur proteins. In addition to biological processes, PCET reactions occur in electrochemical processes and in solid state materials.

Recently a number of experiments on model PCET systems have been performed. Nocera and co-workers have performed experiments in which they photoinduced electron transfer within an electron donor−acceptor pair connected by a proton transfer interface.[3−5] Meyer and co-workers,[6] as well as Farrer and Thorp,[7] have studied proton-coupled electron transfer in oxoruthenium polypyridyl complexes and in some cases have measured unusually large deuterium kinetic isotope effects. Mayer and co-workers[8] have obtained mechanistic evidence for concerted PCET in self-exchange reactions between biimidazoline iron complexes. These types of experimental studies on model PCET systems are becoming more prevalent as the important role of PCET in chemistry and biology is recognized.

Theoretical formulations for single electron transfer (ET) and single proton transfer (PT) reactions in solution have been discussed throughout the literature.[9−14] In the most basic approach, a single charge transfer reaction in a polar solvent is described in terms of two diabatic states corresponding to the charge localized on either its donor or its acceptor. The free energy surfaces are obtained as functions of a single collective solvent reaction coordinate, corresponding to the difference in interaction energies of the two diabatic states with the solvent polarization. For single ET reactions, these free energy surfaces represent the two electronic states and are typically parabolic. For single PT reactions, the transferring hydrogen nucleus is treated quantum mechanically, and these free energy surfaces represent the proton vibrational states. In either case, the charge transfer reaction requires a reorganization of the solvent from the equilibrium reactant to the equilibrium product configuration. The effects of intramolecular solute modes have also been incorporated into this basic formulation.[10] Rate expressions have been derived for various limits, including small and large coupling between the two diabatic states. These theoretical descriptions of single charge transfer reactions have been successfully applied to a wide range of reactions in solution and proteins and have been extended to study multiple electron transfer reactions.[15]

A number of additional challenges arise in the development of a theory for PCET reactions. Such a theory must accurately describe a wide range of time scales. These time scales include the solute electrons involved in PT (i.e., the breaking and forming of bonds), the solute electrons involved in ET, the transferring proton(s), and the solvent electronic and nuclear polarization. In addition to this wide range of time scales, the quantum mechanical behavior of both electrons and protons must be incorporated into a theoretical formulation for PCET. Quantum mechanical effects such as zero point energy, hydrogen tunneling, and transitions between electronic and proton vibrational states have been found to play important roles. In addition, a theory for PCET must include all of the couplings involved in these types of reactions. The solvent is coupled to both the electron and the proton, and the electron and proton are coupled to each other. As a result of these complexities, the theory of PCET has not been developed as extensively as the theory of single ET or single PT. To date, two distinct theoretical formulations for PCET have been proposed. The first was developed by Cukier and co-workers,[3,16] and the second was developed by Hammes-Schiffer and co-workers.[17−20] This Account centers on the second theoretical formulation, although a brief discussion of the first formulation will be presented for comparison.

In the theory for PCET developed by Hammes-Schiffer and co-workers,[17−20] a PCET reaction involving the transfer

Sharon Hammes-Schiffer received her B.A. from Princeton University in 1988 and her Ph.D. from Stanford University in 1993. Following a two-year postdoctoral appointment with John Tully at AT&T Bell Laboratories, she accepted a position as the Clare Boothe Luce Assistant Professor of Chemistry at the University of Notre Dame. Recently she was appointed the Shaffer Associate Professor of Chemistry at The Pennsylvania State University. Her research centers on the theoretical and computational investigation of proton, hydride, and proton-coupled electron transfer reactions in solution and enzymes.

* E-mail: shs@chem.psu.edu.

10.1021/ar9901117 CCC: $20.00
Published on Web 00/00/0000

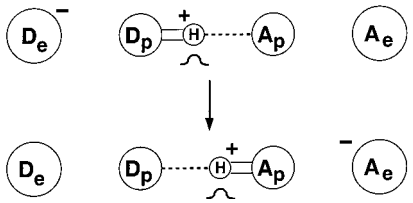

FIGURE 1. Schematic illustration of a PCET reaction, where the electron donor and acceptor are denoted D_e and A_e, respectively, and the proton donor and acceptor are denoted D_p and A_p, respectively. The transferring proton is represented as both a sphere and a quantum mechanical wave function.

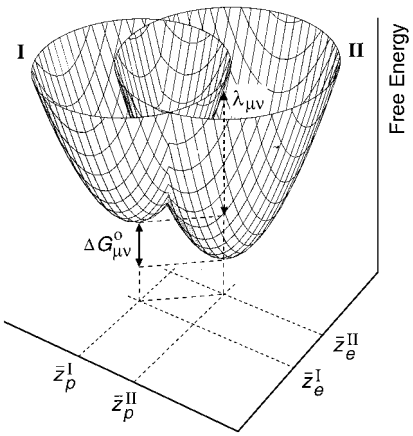

FIGURE 2. Schematic illustration of a pair of paraboloids Iμ and IIν as functions of the solvent coordinates z_p and z_e. The reorganization energy $\lambda_{\mu\nu}$ and the equilibrium free energy difference $\Delta G^{\circ}_{\mu\nu}$ are indicated.

of one electron and one proton (depicted in Figure 1) is described in terms of four diabatic states.[17] These four charge transfer states correspond to the following: the proton and electron on their donors, the proton and electron on their acceptors, the proton on its donor and the electron on its acceptor, and the proton on its acceptor and the electron on its donor. The transferring hydrogen nucleus is treated quantum mechanically to include effects such as zero point energy and hydrogen tunneling. Within this four-state model, the mixed electronic/proton vibrational free energy surfaces are obtained as functions of two collective solvent coordinates corresponding to ET and PT. Often the free energy surfaces for PCET reactions may be approximated as two-dimensional paraboloids (i.e., bowl-shaped surfaces), as illustrated in Figure 2. In this case, the PCET reaction may be viewed as a transition from the reactant set of paraboloids to the product set of paraboloids. Thus, this theory is a multidimensional analogue of standard Marcus theory for single ET involving one-dimensional parabolas.[9] As for single charge transfer, the PCET reaction requires a reorganization of the solvent from the equilibrium reactant to the equilibrium product configuration. The effects of intramolecular solute modes have also been incorporated into this formulation. This Account will summarize this theoretical formulation of PCET and will discuss recent applications to chemical systems.

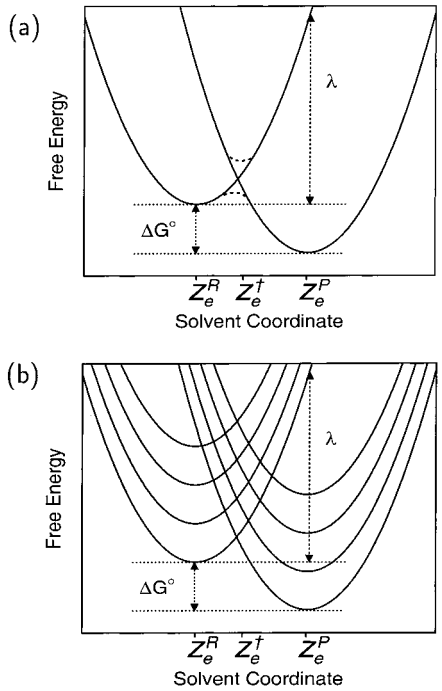

FIGURE 3. (a) Schematic illustration of the diabatic (solid) and adiabatic (long-dashed) electronic free energy curves as functions of the solvent coordinate z_e for a single electron transfer reaction. The Marcus theory quantities ΔG° and λ are indicated. (b) Same as (a) but including the intramolecular solute vibrational states (assumed to be harmonic and uncoupled to the solvent).

Theory

Single Charge Transfer Reactions. Single ET reactions are often described in terms of two diabatic states:

$$(1) \qquad D_e^{\ominus} \quad A_e$$

$$(2) \qquad D_e \quad A_e^{\ominus}$$

where D_e and A_e indicate the electron donor and acceptor, respectively. In standard Marcus theory for ET in polar solvents, the energies of these diabatic states are parabolic functions of a collective solvent coordinate z_e. A schematic picture of the energies of the diabatic states is shown in Figure 3a. The solvent coordinate z_e represents the difference in the interaction energies of the two diabatic states with the solvent inertial polarization. (In this Account the solvent electrons are assumed to respond instantaneously to the solute electrons, and the solvent inertial polarization refers to the noninstantaneous solvent response, including nuclear reorientation and translation.) In this theoretical framework, the ET reaction requires a reorganization of the solvent (i.e., outer-sphere reorganization) from the equilibrium reactant configuration z_e^R to the equilibrium product configuration z_e^P. Rate expressions have been derived in both the adiabatic and nonadiabatic limits of ET, where electronically adiabatic refers to the limit in which the solute electrons respond instantaneously to the solvent inertial polarization. (Typically a reaction is electronically adiabatic when the coupling between the two diabatic states is much larger than the thermal energy and is electronically nonadiabatic

when this coupling is much smaller than the thermal energy.)

This theory of ET has been extended to include the effects of intramolecular solute modes (i.e., inner-sphere reorganization). In this case, the vibrational wave functions corresponding to the relevant solute modes are calculated for each diabatic state. If these solute modes are not coupled to the solvent, the vibrational states corresponding to each electronic diabatic state are parabolas with the same minimum and frequency but shifted upward in energy. Figure 3b depicts these vibrational states for the simple case of a single vibrational solute mode that is harmonic and not coupled to the solvent. In the limit of nonadiabatic ET, the Golden Rule may be used to derive a rate expression for nonadiabatic transitions from the reactant set of vibrational states to the product set of vibrational states:[10,12]

$$k_{12} = \frac{2\pi}{\hbar}|V_{12}|^2(4\pi\lambda k_B T)^{-1/2} \times \sum_\mu P_{1\mu} \sum_\nu S^2_{1\mu,2\nu} \exp\left\{\frac{-(\Delta G^\circ_{1\mu,2\nu} + \lambda)^2}{4\lambda k_B T}\right\} \quad (1)$$

where $\sum_\mu$ and $\sum_\nu$ indicate summations over the vibrational states for diabatic states 1 and 2, respectively, V_{12} is the coupling between the two diabatic states, λ is the reorganization energy, $S_{1\mu,2\nu}$ is the overlap of the vibrational wave functions 1μ and 2ν, $\Delta G^\circ_{1\mu,2\nu}$ is the equilibrium free energy difference between solvated vibrational states 1μ and 2ν, and $P_{1\mu}$ is the Boltzmann factor for state 1μ. The various quantities in this rate expression may be measured experimentally[10] or determined computationally with electronic structure calculations, dielectric continuum theory,[21,22] and in some cases molecular dynamics simulations. Note that this rate expression was derived for the case of no coupling between the solute mode and the solvent. As a result, it is not generally applicable to PCET reactions in which the motion of the transferring proton (which is coupled to polar solvents) is identified as the relevant solute mode.

Single PT reactions may also be described in terms of two diabatic states:

$$(a) \quad D_pH^\oplus \quad A_p$$

$$(b) \quad D_p \quad {}^\oplus HA_p$$

where D_p and A_p indicate the proton donor and acceptor, respectively. As for ET reactions, single PT reactions in polar solvents may be described in terms of a collective solvent coordinate z_p, which represents the difference in interaction energies of the two diabatic states with the solvent inertial polarization. The additional complication that arises for single PT reactions is the motion of the transferring hydrogen nucleus, which must be treated quantum mechanically. This discussion will focus on electronically adiabatic proton transfer since this is the relevant limit for PCET reactions involving hydrogen bonding at the proton transfer interface. Within the valence bond description, the lowest electronically adiabatic free energy surface $E_g(r_p,z_p)$ is obtained by diagonalization of the Hamiltonian matrix in the basis of the two diabatic states. The proton vibrational wave functions may be calculated for the proton moving in the potential energy $E_g(r_p,z_p)$ for each fixed solvent coordinate z_p, resulting in free energy surfaces $\epsilon_\mu(z_p)$ that are functions of only the solvent coordinate z_p.[17]

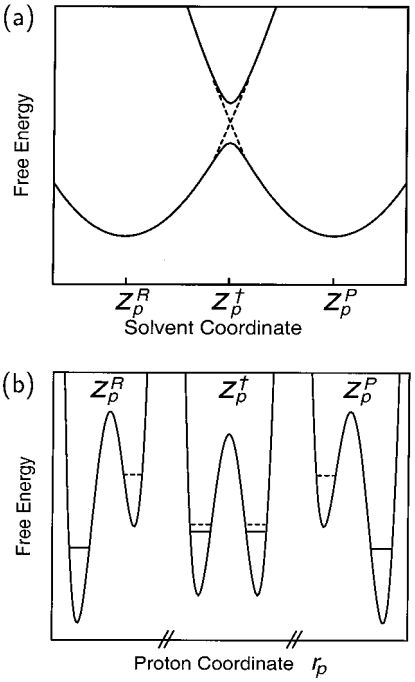

FIGURE 4. (a) Schematic illustration of the adiabatic (solid) and diabatic (dashed) vibrational free energy curves as functions of the solvent coordinate z_p for a symmetric single proton transfer reaction. (b) Proton potential energy curves as functions of the proton coordinate r_p for three specific values of the solvent coordinate z_p indicated in (a).

Figure 4a depicts the two lowest energy vibrational surfaces for a symmetric proton transfer reaction. Note that these surfaces resemble the adiabatic free energy surfaces calculated for single ET reactions shown in Figure 3a. As for ET, the PT reaction involves a reorganization of the solvent from the equilibrium reactant to the equilibrium product configuration. In the case of PT, however, these free energy surfaces represent proton vibrational states. Figure 4b depicts the proton potential energy curves $E_g(r_p,z_p)$ and the corresponding proton vibrational wave functions for three different solvent coordinates. Note that the solvent polarization impacts the shape of the proton potential energy curve, particularly the relative energies of the reactant and product wells. For the equilibrium reactant solvent configuration, the *a* well is lower in energy, and the lowest energy vibrational wave function is localized in the *a* well. For the equilibrium product solvent configuration, the *b* well is lower in energy, and the lowest energy vibrational wave function is localized in the *b* well. At the crossing point, the *a* and *b* wells are degenerate, and the lowest energy vibrational wave function is delocalized between the two wells. The energy difference between the two lowest energy vibra-

tional states at this point is the tunnel splitting, which determines the probability of hydrogen tunneling. In general, PT reactions may be vibrationally adiabatic (with large tunnel splittings), vibrationally nonadiabatic (with small tunnel splittings), or in the intermediate regime. The vibrationally adiabatic limit corresponds to the instantaneous response of the transferring proton to the solvent inertial polarization.

To summarize the theoretical description of single charge transfer reactions in polar solvents, typically they may be described in terms of two diabatic states and a single collective solvent coordinate.

Fundamental Aspects of Proton-Coupled Electron Transfer. As described in ref 17, the theoretical description of the most basic PCET reaction involving the transfer of one electron and one proton requires four diabatic states:

$$(1a) \qquad D_e^{\ominus}-{}^{\oplus}D_pH\cdots\ \cdots A_p-A_e$$

$$(1b) \qquad D_e^{\ominus}-D_p\cdots\ \cdots HA_p^{\oplus}-A_e$$

$$(2a) \qquad D_e-{}^{\oplus}D_pH\cdots\ \cdots A_p-A_e^{\ominus}$$

$$(2b) \qquad D_e-D_p\cdots\ \cdots HA_p^{\oplus}-A_e^{\ominus}$$

The notation for these diabatic states is consistent with the notation used in the above discussion of single ET and single PT. Thus, "1" and "2" indicate the ET states, and "*a*" and "*b*" indicate the PT states. If the initial state is 1*a*, a transition to 1*b* corresponds to PT, a transition to 2*a* corresponds to ET, and a transition to 2*b* corresponds to EPT (in which both the electron and the proton transfer). The free energy surfaces are obtained as functions of two solvent coordinates z_p and z_e corresponding to the PT and ET reactions, respectively. Each scalar solvent coordinate represents the difference in interaction energy of the two diabatic states involved in the charge transfer reaction with the solvent inertial polarization. Note that this theory is simply a multidimensional generalization of Marcus theory for single charge transfer, where each solvent coordinate is analogous to that used to describe a single ET or single PT reaction.

There are three distinct regimes of PCET:

1. Electronically adiabatic PT and ET, where the coupling between all pairs of the four diabatic states is strong. In this adiabatic regime, the system evolves on the lowest two-dimensional mixed electronic/proton vibrational free energy surface.[17] This surface could have up to four minima, and the rate for transitions between minima could be calculated using the multidimensional generalization of the Grote−Hynes theory.[23]

2. Electronically nonadiabatic PT and ET, where the coupling between all pairs of the four diabatic states is weak. In this case, the system can be viewed in terms of electronically diabatic vibrational surfaces determined by calculating the proton vibrational states for each electronically diabatic state. The resulting diabatic free energy surfaces may be approximated as four sets of shifted paraboloids (with identical frequencies) in the two-dimensional solvent space. Analogous to Marcus theory for nonadiabatic single ET, the Golden Rule can be applied to calculate the rate for transitions among these electronically diabatic states.

3. Electronically adiabatic PT and electronically nonadiabatic ET, where the coupling between PT diabatic states is strong and the coupling between ET diabatic states is weak. In this case, the four-state model can be reduced to a two-state model, and the system can be viewed in terms of two sets of ET diabatic states. The ET diabatic free energy surfaces are approximate paraboloids, and in the limit of small coupling the Golden Rule can be used to calculate the rate of transitions between the two sets of approximate paraboloids.

The regime of electronically adiabatic PT and electronically nonadiabatic ET is most relevant for PCET reactions with a well-separated electron donor and acceptor connected by a hydrogen-bonded interface. For this reason the remainder of this discussion will focus on this regime. The ET diabatic free energy surfaces may be calculated with a multistate continuum theory[17] or with molecular dynamics simulations including explicit solvent molecules. In either case, the ET diabatic free energy surfaces may be calculated in two steps. In the first step, the lowest energy electronically adiabatic PT state is calculated for each ET state. The free energies of these two states are denoted $E_g^{I}(r_p,z_p,z_e)$ (corresponding to a mixture of 1*a* and 1*b*) and $E_g^{II}(r_p,z_p,z_e)$ (corresponding to a mixture of 2*a* and 2*b*). In the second step, the proton vibrational wave functions are calculated for each of these two ET states. The energies of the resulting vibrational states are denoted $\epsilon_\mu^{I}(z_p,z_e)$ and $\epsilon_\nu^{II}(z_p,z_e)$, corresponding to ET states 1 and 2, respectively. Typically these ET diabatic free energy surfaces may be approximated as two sets of "paraboloids" with identical frequencies. The minima within each set of paraboloids are slightly shifted due to different weightings of the *a* and *b* PT states.

Figure 5a depicts the ET diabatic free energy surfaces as functions of the two solvent coordinates for a model PCET reaction. The reactants (I) are mixtures of the 1*a* and 1*b* diabatic states, and the products (II) are mixtures of the 2*a* and 2*b* diabatic states. Only the two lowest energy ET diabatic surfaces are shown for the reactants and the products, and they are each labeled according to the dominant diabatic state. Note that the minima within the reactants and products are shifted since different weightings of the *a* and *b* PT states result in different equilibrium solvent configurations. Also note that the range for the z_e coordinate is significantly larger than the range for the z_p coordinate. This disparity between the ranges of the two solvent coordinates is caused by the much larger reorganization energy (due to the larger donor−acceptor distance) for ET than for PT. The analysis of these two-dimensional free energy surfaces may be simplified by investigating one-dimensional slices. For example, Figure 5b depicts a one-dimensional slice that connects the minima of the lowest energy reactant and product surfaces shown in Figure 5a. Note that the solvent

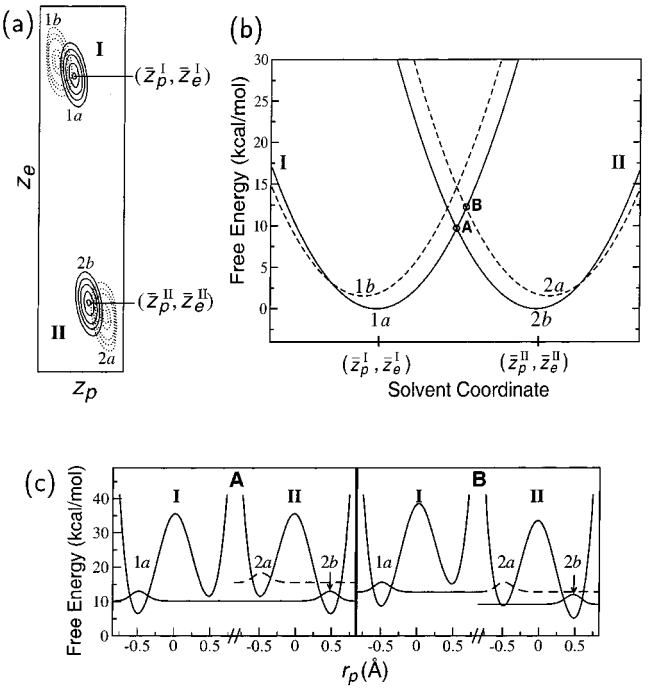

FIGURE 5. (a) Schematic illustration of two-dimensional ET diabatic mixed electronic/proton vibrational free energy surfaces as functions of the solvent coordinates z_p and z_e. The reactant and product ET diabatic surfaces are labeled I and II, respectively. Only two surfaces are shown for each ET diabatic state, and the lower and higher energy surfaces are shown with solid and dashed contour lines, respectively. Each free energy surface is labeled according to the dominant diabatic state, and the minima of the lowest surfaces are labeled $(\bar{z}^{I}_{p},\bar{z}^{I}_{e})$ and $(\bar{z}^{II}_{p},\bar{z}^{II}_{e})$. (b) Slices of the free energy surfaces along the straight-line reaction path connecting solvent coordinates $(\bar{z}^{I}_{p},\bar{z}^{I}_{e})$ and $(\bar{z}^{II}_{p},\bar{z}^{II}_{e})$ indicated in (a). Only the lowest surface is shown for the reactant (I), and the lowest two surfaces are shown for the product (II). (c) The reactant (I) and product (II) proton potential energy curves as functions of r_p at the solvent configurations corresponding to the intersection points A and B indicated in (b).

coordinate in this one-dimensional figure is a combination of z_p and z_e.

These mixed electronic/proton vibrational free energy surfaces may be further analyzed by investigating the associated proton potential energy curves and proton vibrational wave functions. Figure 5c depicts the proton potential energy curves and the proton vibrational wave functions associated with the solvent coordinates of the two intersection points for the free energy surfaces shown in Figure 5b. For the solvent coordinates representing the intersection of the reactant 1*a* and the product 2*b* surfaces, the reactant proton vibrational state localized in the *a* well is degenerate with the product proton vibrational state localized in the *b* well. For the solvent coordinates representing the intersection of the reactant 1*a* and the product 2*a* surfaces, the reactant proton vibrational state localized in the *a* well is degenerate with the product proton vibrational state localized in the *a* well. These figures illustrate that the proton is transferred during the transition from the 1*a* to the 2*b* surface but is not transferred during the transition from the 1*a* to the 2*a* surface at the intersection points. Thus, the transition from 1*a* to 2*b* corresponds to EPT, where both the electron and the proton are transferred, while the transition from 1*a* to 2*a* corresponds to ET, where only the electron is transferred.

This theoretical framework encompasses both concerted and sequential PCET reactions, as illustrated in Figure 5a. A concerted PCET reaction involves a direct transition from 1*a* to 2*b*. A sequential PCET reaction involves either a transition from 1*a* to 1*b* followed by a transition from 1*b* to 2*b* (PT followed by ET) or a transition from 1*a* to 2*a* followed by a transition from 2*a* to 2*b* (ET followed by PT). As shown in Figure 6, the PT reaction in a sequential mechanism may be vibrationally adiabatic or nonadiabatic. The rate expression in eq 2 may be applied to systems that exhibit either vibrationally adiabatic or vibrationally nonadiabatic PT as long as the surfaces are still approximate paraboloids and the appropriate representation (i.e., vibrationally adiabatic or vibrationally diabatic) is chosen.[20]

Although all of these mechanisms may be described within this theoretical framework, many reactions are in the intermediate regime between concerted and sequential. In fact, since the electrons and transferring proton are quantum mechanical wave functions (i.e., delocalized) in this theoretical formulation, a strictly sequential or concerted reaction is not clearly defined (unless an intermediate is observed experimentally). Note that, within this theoretical formulation, hydrogen atom transfer may be defined loosely as concerted EPT for a system in which the proton donor and acceptor are the same as the electron donor and acceptor. Such hydrogen atom transfer reactions are expected to be electronically adiabatic (due to the shorter electron donor−acceptor distance) and to be dominated more by intramolecular solute modes than by solvent reorganization (due to the smaller change in the dipole moment).

Rate Expression. Soudackov and Hammes-Schiffer have derived a rate expression in the limit of electronically adiabatic PT and electronically nonadiabatic ET.[19] Application of the Golden Rule to the two sets of free energy surfaces illustrated in Figure 5a (approximated as paraboloids with identical frequencies) leads to the following rate expression:[19]

$$k = \frac{2\pi}{\hbar}\sum_{\mu} P_{\mathrm{I}\mu} \sum_{\nu} V^{2}_{\mu\nu} (4\pi\lambda_{\mu\nu} k_{\mathrm{B}} T)^{-1/2} \exp\left\{\frac{-(\Delta G^{\circ}_{\mu\nu} + \lambda_{\mu\nu})^{2}}{4\lambda_{\mu\nu} k_{\mathrm{B}} T}\right\} \tag{2}$$

where $\sum_{\mu}$ and $\sum_{\nu}$ indicate a sum over vibrational states associated with ET states 1 and 2, respectively, and $P_{\mathrm{I}\mu}$ is the Boltzmann factor for state Iμ. In this expression the reorganization energy is defined as

$$\lambda_{\mu\nu} = \epsilon^{\mathrm{I}}_{\mu}(\bar{z}^{\mathrm{II}\nu}_{\mathrm{p}},\bar{z}^{\mathrm{II}\nu}_{\mathrm{e}}) - \epsilon^{\mathrm{I}}_{\mu}(\bar{z}^{\mathrm{I}\mu}_{\mathrm{p}},\bar{z}^{\mathrm{I}\mu}_{\mathrm{e}}) = \epsilon^{\mathrm{II}}_{\nu}(\bar{z}^{\mathrm{I}\mu}_{\mathrm{p}},\bar{z}^{\mathrm{I}\mu}_{\mathrm{e}}) - \epsilon^{\mathrm{II}}_{\nu}(\bar{z}^{\mathrm{II}\nu}_{\mathrm{p}},\bar{z}^{\mathrm{II}\nu}_{\mathrm{e}}) \tag{3}$$

and the free energy difference is defined as

$$\Delta G^{\mathrm{o}}_{\mu\nu} = \epsilon^{\mathrm{II}}_{\nu}(\bar{z}^{\mathrm{II}\nu}_{\mathrm{p}},\bar{z}^{\mathrm{II}\nu}_{\mathrm{e}}) - \epsilon^{\mathrm{I}}_{\mu}(\bar{z}^{\mathrm{I}\mu}_{\mathrm{p}},\bar{z}^{\mathrm{I}\mu}_{\mathrm{e}}) \tag{4}$$

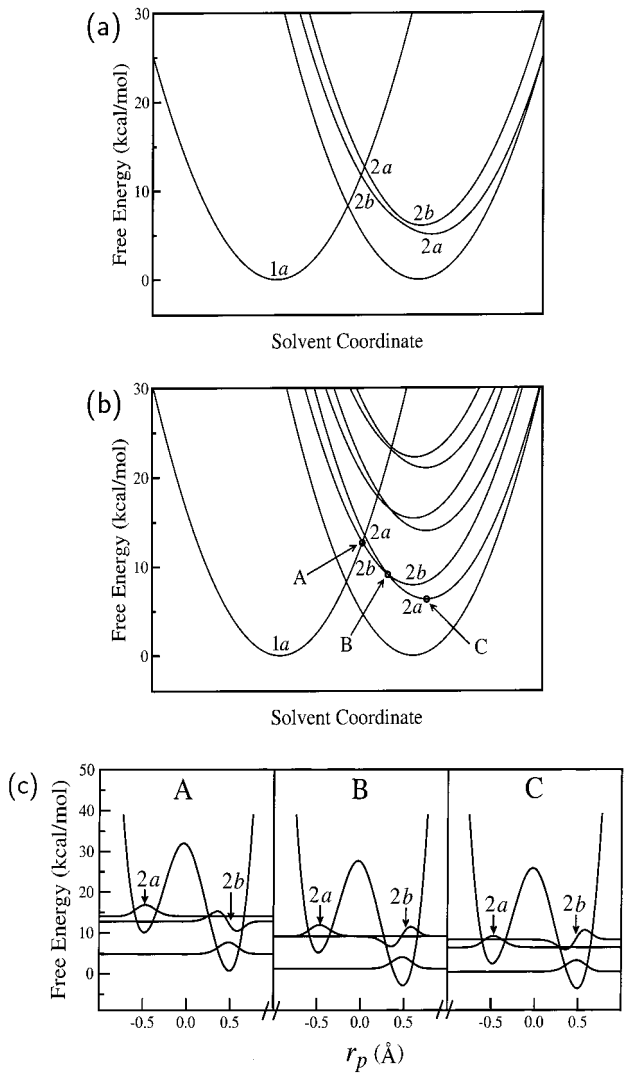

FIGURE 6. (a) Slices of the ET diabatic free energy surfaces along the straight-line reaction path for a model system that is predominantly vibrationally adiabatic. (b) Same as (a) for a model system that is vibrationally nonadiabatic. The lowest reactant and the second and third product ET diabatic surfaces are labeled according to the dominant diabatic state. (c) The product proton potential energy curves at the solvent coordinates corresponding to A, B, and C indicated on the free energy surfaces in (b). The lowest three product proton vibrational wave functions are shown for each potential energy curve, and the second and third ones are labeled according to the dominant diabatic state. Note that at the vibrationally nonadiabatic avoided crossing, a pair of product proton vibrational states becomes nearly degenerate, leading to a change in the dominant diabatic state for the corresponding ET diabatic free energy surfaces.

where $(\bar{z}_p^{I\mu},\bar{z}_e^{I\mu})$ and $(\bar{z}_p^{II\nu},\bar{z}_e^{II\nu})$ are the solvent coordinates for the minima of $\epsilon_\mu^I(z_p,z_e)$ and $\epsilon_\nu^{II}(z_p,z_e)$, respectively. These quantities are illustrated for a pair of paraboloids in Figure 2. The coupling $V_{\mu\nu}$ is defined as a quantity $V(r_p,z_p)$ averaged over the reactant and product proton vibrational wave functions Iμ and IIν, where $V(r_p,z_p)$ is a linear combination of the couplings between the four diabatic states with weightings dependent on the proton coordinate r_p (and assumed to be independent of z_p). As a result of this averaging over the proton vibrational wave functions, typically the coupling $V_{\mu\nu}$ is much smaller than the thermal energy for EPT reactions, even if the associated ET reaction is electronically adiabatic.

Despite obvious similarities, the rate expression given in eq 2 for PCET is fundamentally different than the rate expression given in eq 1 for single ET in the presence of a solute mode uncoupled to the solvent. The most fundamental difference is that the reorganization energies, equilibrium free energy differences, and couplings in eq 2 are defined in terms of two-dimensional paraboloids instead of one-dimensional parabolas. Another important difference is that the reorganization energies $\lambda_{\mu\nu}$ in eq 2 are different for each pair of intersecting ET diabatic surfaces due to the varying positions of the minima within the reactant and product states. In contrast, λ in eq 1 is a constant and is the same for all pairs of intersecting parabolas. The final critical difference is that the coupling $V_{\mu\nu}$ in eq 2 cannot be expressed as the product of a constant coupling and an overlap of the reactant and product vibrational wave functions, as in eq 1.

Cukier and co-workers[3,16] used eq 1 to calculate two separate rates for ET and EPT. Since eq 1 has been derived for a single ET reaction described by a single solvent coordinate z_e with an inner-sphere solute mode that is not coupled to the solvent, the direct application of this equation does not accurately account for the coupling of the proton to the solvent in PCET reactions. A more comprehensive comparison of the theoretical formulation described in this Account to that of Cukier is given in ref 19.

Intramolecular Solute Modes. The effects of intramolecular solute modes (i.e., inner-sphere reorganization) may easily be incorporated within this theoretical framework. Typically, the gas-phase Hamiltonian is parametrized as a function of the relevant solute modes and is fit to either experimental data or electronic structure calculations. The free energy is calculated as a function of the proton coordinate(s), the scalar solvent coordinates, and the intramolecular solute coordinates (assumed to be uncoupled to the solvent). The "slow" solute modes are treated in the same way as the solvent coordinates, so the free energy surfaces are functions of the solvent coordinates and the slow solute mode coordinates. The "fast" solute modes are treated quantum mechanically in the same way as the proton coordinate(s), and the vibrational wave functions depend explicitly on both the proton coordinate(s) and the fast solute mode coordinates.

The extension of the rate expression given in eq 2 to include quantum mechanical harmonic solute modes uncoupled to the solvent and the proton coordinate is derived in ref 19. In general, however, the solute mode may be anharmonic and may be coupled to the proton coordinate in PCET reactions. For example, typically the proton donor−acceptor vibrational mode is significantly coupled to the proton coordinate. In this case, a multidimensional Schrödinger equation including all coupling between vibrational modes must be solved. This approach is straightforward for a reasonably small number of relevant solute modes.

Applications

Required Input Quantities. In this valence bond approach,[14] the gas phase matrix elements are represented by standard molecular mechanical terms fit to electronic structure calculations or experimental data. Typically, the solvent−solvent and solvent−solute interactions are added to the diagonal elements of the gas phase Hamiltonian matrix. When the solvent is treated as a dielectric continuum, the solvent reorganization energy matrix elements may be determined with standard electrostatic continuum methods[21] or more elaborate two-cavity models.[22] When the solvent is treated explicitly with molecular dynamics simulations, the solvent−solvent and solvent−solute interactions are described with standard molecular mechanical potential energy terms such as Coulomb and Lennard-Jones interactions.

Systematic Model Studies. To elucidate the fundamental principles of PCET, Decornez and Hammes-Schiffer applied this theoretical formulation of PCET to a series of simple model systems consisting of an electron donor and acceptor connected by a protonated water dimer.[20] These model systems resemble Figure 1, where D_p and A_p are represented as water molecules (in an orientation ensuring a symmetric proton transfer interface) and D_e and A_e are represented as point charges. This solute is placed in an ellipsoidal cavity embedded in a dielectric continuum solvent. This systematic study resulted in predictions of the dependence of the rates, mechanisms, and kinetic isotope effects on the physical properties of the solute and the solvent. The physical properties varied in this study included the proton donor−acceptor distance, the electron donor−acceptor distance, the exothermicity (or endothermicity) of the PT and ET reactions, the temperature, the solvent polarity, and the size of the electron donor and acceptor.

The mechanism of a PCET reaction is determined by a competition between the couplings (which typically favor ET) and the free energy barriers (which typically favor EPT for symmetric proton transfer interfaces). The couplings tend to favor ET due to averaging over the reactant and product proton vibrational wave functions. As shown in Figure 5c, for EPT the reactant and product proton vibrational wave functions are localized in different wells of the proton potential energy curve, while for ET these wave functions are both localized in the same well. Thus, the overlap between the reactant and product proton vibrational wavefunctions is much smaller for EPT than for ET, leading to a smaller coupling for EPT. The free energy barriers tend to favor EPT for symmetric proton transfer interfaces in which the electron and proton are transferring in the same direction due to the attractive electrostatic interaction between the transferring proton and electron. As a result of this interaction, the 2*b* diabatic state is lower in energy than the 2*a* diabatic state, leading to a lower free energy barrier for EPT. Altering the physical properties of the solute and the solvent impacts the competition between the couplings and the free energy barriers and thus determines the mechanism. The effects of specific physical properties on the mechanisms and rates of these types of PCET reactions are presented in ref 20.

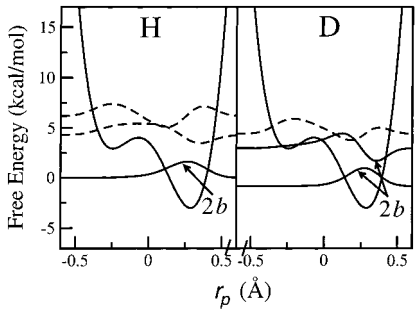

FIGURE 7. Product proton potential energy curve and the associated product proton vibrational wave functions for a model system with hydrogen and deuterium. The localized wave functions are denoted by solid lines and are labeled according to the dominant diabatic state, while the delocalized wave functions are denoted by dashed lines.

The dependence of the kinetic isotope effects (i.e., the ratio of the rate with hydrogen to the rate with deuterium) on the physical properties of PCET systems was also investigated in ref 20. Figure 7 illustrates the vibrational wave functions for hydrogen and deuterium for a product proton potential energy curve. Although the proton-transfer interface is symmetric for this model system, the proton potential energy curve is asymmetric due to the electrostatic interaction between the transferring proton and electron. (For the product ET diabatic state the electron is on the acceptor, lowering the energy of the PT diabatic state *b* with the proton on its acceptor.) As expected, the zero point energy and the splittings between energy levels are smaller for deuterium than for hydrogen. In addition, the qualitative characteristics of the second vibrational wave functions differ significantly for deuterium and hydrogen: for deuterium the second state is below the barrier and localized in the *b* well, while for hydrogen the second state is slightly above the barrier and delocalized. These types of differences between hydrogen and deuterium could lead to substantial mechanistic differences. As a result, the analysis of the kinetic isotope effects for PCET reactions may be complex.

In general, the kinetic isotope effect of a PCET reaction will increase as the probability of the EPT mechanism increases and as the localization of and distance between the reactant and product proton vibrational wave functions increase. The reactant and product proton vibrational wave functions become more localized and separated as the proton donor−acceptor distance increases (leading to higher and wider PT barriers) and as the electron donor−acceptor distance decreases (leading to stronger electron−proton electrostatic interactions). Note that the probability of EPT becomes smaller, while the separation between the vibrational wave functions becomes higher, as the proton donor−acceptor distance increases. As a result, the kinetic isotope effects are largest for intermediate proton donor−acceptor distances. In some cases, unusually large kinetic isotope effects may

be observed for systems in which the EPT mechanism dominates. These large kinetic isotope effects are due to the electron−proton electrostatic interaction, which leads to proton vibrational wave functions that are highly localized near the proton donor or acceptor.

PCET through Asymmetric Salt Bridges. The initial application of this theoretical formulation for PCET was the investigation of PCET through asymmetric salt bridges.[18] A comparative study was performed for PCET within a donor−(amidinium−carboxylate)−acceptor salt bridge and the corresponding switched inteface donor−(carboxylate−amidinium)−acceptor salt bridge. These theoretical investigations were motivated by experiments reported by Nocera and co-workers, who studied photoinduced PCET from a Ru(II) polypyridine complex to a dinitrobenzene through amidinium−carboxylate (and carboxylate−amidinium) salt bridges.[5] These experiments indicate that the rate of electron transfer is $\sim 10^2$ faster for the carboxylate−amidinium interface than for the amidinium−carboxylate interface. The calculations presented in ref 18 are qualitatively consistent with these experimental results and provide insight into the chemical and physical basis for this difference in rates.

Conclusions

This Account summarizes a comprehensive theoretical formulation for PCET reactions. In this theory, the active electrons and transferring protons are treated quantum mechanically. In the most basic form, the solute is described in terms of four diabatic states representing the charge transfer states for a proton and an electron transfer. The free energy surfaces are obtained as functions of two collective solvent coordinates corresponding to the proton and electron transfer reactions. These surfaces provide important information about the reaction mechanisms, such as whether the proton and electron transfer reactions are concerted or sequential and, in the latter case, the order in which these reactions occur. Rate expressions have been derived in the various limits. The nuclear quantum effects of the transferring hydrogen and the effects of intramolecular solute modes have been incorporated into this theoretical formulation.

The application of this theoretical formulation for PCET reactions is straightforward. The gas phase Hamiltonian matrix elements may be represented as molecular mechanical terms fit to electronic structure calculations or experimental data. Within the dielectric continuum treatment of the solvent, the solvent reorganization energy matrix elements may be calculated with standard electrostatic continuum methods. The solvent may also be treated explicitly in conjunction with molecular dynamics simulations. Systematic model studies have been conducted to predict the dependence of the rates, mechanisms, and kinetic isotope effects on the physical properties of the solute and the solvent. In addition, this theoretical formulation has been applied to experimentally studied photoinduced PCET through asymmetric salt bridges.

This theoretical formulation has been extended to study processes involving the transfer of multiple protons and multiple electrons. Processes involving N charge transfer reactions may be described in terms of 2^N diabatic states, and the free energy surfaces are functions of N collective solvent coordinates. For example, recently the previous application of this theory to PCET through asymmetric salt bridges[18] was extended to include the possibility of an additional PT reaction at the proton transfer interface (i.e., two PT reactions and one ET reaction). In this study, the PCET reaction was described by eight diabatic states and three collective solvent coordinates.

Methodology has also been developed to include dynamical effects of the solvent or protein within this theoretical framework.[24,25] The molecular dynamics with quantum transitions (MDQT) surface hopping method is used to incorporate transitions among the mixed electronic/proton vibrational states. This approach is advantageous in that it is valid in the adiabatic and nonadiabatic limits and in the intermediate regime. In addition, this approach provides real-time dynamical information on a molecular level. This dynamical MDQT approach has already been applied to one-dimensional model PCET systems.[24]

The critical role of PCET reactions in chemistry and biology is continuing to be discovered. Experiments on model PCET systems are becoming more prevalent. The theoretical formulation described in this Account provides a framework for the analysis of these experimental results and for the prediction of trends that may be tested experimentally. The interplay between experiment and theory will be vital to the elucidation of the underlying fundamental principles of PCET reactions.

I owe great thanks to Hélène Decornez and Alexander Soudackov for useful discussions about PCET. I am also very grateful to Hélène Decornez for making all of the figures in this Account. This work has been supported by the NSF CAREER program Grant CHE-9623813 and the NIH Grant GM56207, as well as an Alfred P. Sloan Foundation Research Fellowship and a Camille Dreyfus Teacher-Scholar Award.

References

(1) Okamura, M. Y.; Feher, G. Proton transfer in reaction centers from photosynthetic bacteria. *Annu. Rev. Biochem.* **1992**, *61*, 861.
(2) Babcock, G. T.; Wikstrom, M. Oxygen activation and the conservation of energy in cell respiration. *Nature* **1992**, *356*, 301.
(3) Cukier, R. I.; Nocera, D. G. Proton-coupled electron transfer. *Annu. Rev. Phys. Chem.* **1998**, *49*, 337.
(4) Turro, C.; Chang, C. K.; Leroi, G. E.; Cukier, R. I.; Nocera, D. G. Photoinduced electron transfer mediated by a hydrogen-bonded interface. *J. Am. Chem. Soc.* **1992**, *114*, 4013.
(5) Kirby, J. P.; Roberts, J. A.; Nocera, D. G. Significant effect of salt bridges on electron transfer. *J. Am. Chem. Soc.* **1997**, *119*, 9230.
(6) Binstead, R. A.; Moyer, B. A.; Samuels, G. J.; Meyer, T. J. Proton-coupled electron transfer between $[Ru(bpy)_2(py)OH_2]^{2+}$ and $[Ru(bpy)_2(py)O]^{2+}$: a solvent isotope effect (H_2O/D_2O) of 16.1. *J. Am. Chem. Soc.* **1981**, *103*, 2897.
(7) Farrer, B. T.; Thorp, H. H. Driving force and isotope dependence of the kinetics of proton-coupled electron transfer in oxoruthenium(IV) polypyridyl complexes. *Inorg. Chem.* **1999**, *38*, 2497.
(8) Roth, J. P.; Lovel, S.; Mayer, J. M. Intrinsic barriers for electron and hydrogen atom transfer reactions of biomimetic iron complexes. *J. Am. Chem. Soc.* **2000**, *122*, 5486.
(9) Marcus, R. A. Chemical and electrochemical electron-transfer theory. *Annu. Rev. Phys. Chem.* **1964**, *15*, 155.

(10) Bixon, M.; Jortner, J. *Electron transfer—from isolated molecules to biomolecules*; Advances in Chemical Physics 106; Pritogine, I., Rice, S. A., Eds.; John Wiley & Sons: New York, 1999; p 35.
(11) Basilevsky, M. V.; Chudinov, G. E.; Newton, M. D. The multiconfigurational adiabatic electron transfer theory and its invariance under transformations of charge density basis functions. *Chem. Phys.* **1994**, *179*, 263.
(12) Barbara, P. F.; Meyer, T. J.; Ratner, M. A. Contemporary issues in electron transfer research. *J. Phys. Chem.* **1996**, *100*, 13148.
(13) Borgis, D.; Hynes, J. T. Dynamical Theory of Proton Tunneling Transfer Rates in Solution: General Formulation. *Chem. Phys.* **1993**, *170*, 315.
(14) Warshel, A. *Computer Modeling of Chemical Reactions in Enzymes and Solutions*; John Wiley: New York, 1991.
(15) Zusman, L. D.; Beratan, D. N. Two-electron transfer reactions in polar solvents. *J. Chem. Phys.* **1996**, *105*, 165.
(16) Cukier, R. I. Proton-coupled electron transfer reactions: Evaluation of rate constants. *J. Phys. Chem.* **1996**, *100*, 15428.
(17) Soudackov, A. V.; Hammes-Schiffer, S. Multistate continuum theory for multiple charge transfer reactions in solution. *J. Chem. Phys.* **1999**, *111*, 4672.
(18) Soudackov, A. V.; Hammes-Schiffer, S. Theoretical study of photoinduced proton-coupled electron transfer through asymmetric salt bridges. *J. Am. Chem. Soc.* **1999**, *121*, 10598.
(19) Soudackov, A. V.; Hammes-Schiffer, S. Derivation of rate expressions for nonadiabatic proton-coupled electron transfer reactions in solution. *J. Chem. Phys.* **2000**, *113*, 2385.
(20) Decornez, H.; Hammes-Schiffer, S. Model proton-coupled electron transfer reactions in solution: prediction of rates, mechanisms, and kinetic isotope effects. *J. Phys. Chem.* **2000**, *104*, 9370.
(21) Tomasi, J.; Persico, M. Molecular interactions in solution—an overview of methods based on continuous distributions of the solvent. *Chem. Rev.* **1994**, *94*, 2027.
(22) Newton, M. D.; Basilevsky, M. V.; Rostov, I. V. A Frequency-Resolved Cavity Model (FRCM) for Treating Equilibrium and Non-Equilibrium Solvation Energies. 2. Evaluation of Solvent Reorganization Energies. *Chem. Phys.* **1998**, *232*, 201.
(23) Hanggi, P.; Talkner, P.; Borkovec, M. Reaction-rate theory: fifty years after Kramers. *Rev. Mod. Phys.* **1990**, *62*, 251.
(24) Fang, J.-Y.; Hammes-Schiffer, S. Proton-coupled electron transfer reactions in solution: molecular dynamics with quantum transitions for model systems. *J. Chem. Phys.* **1997**, *106*, 8442.
(25) Hammes-Schiffer, S. Mixed quantum/classical dynamics of hydrogen transfer reactions. *J. Phys. Chem. A* **1998**, *102*, 10443.

AR9901117